Journal of Alloys and Compounds 502 (2010) 153–157

Contents lists available at ScienceDirect

Journal of Alloys and Compounds

journal homepage: www.elsevier.com/locate/jallcom

New dielectric material system of xLa($Mg_{1/2}Ti_{1/2}$)O_3–(1 − x)$Ca_{0.61}Nd_{0.8/3}TiO_3$ at microwave frequency

Yuan-Bin Chen*

Department of Engineering & Management of Advanced Technology, Chang Jung Christian University, 396 Chang Jung Road, Sec. 1, Kway Jen, Tainan 71101, Taiwan

ARTICLE INFO

Article history:
Received 17 March 2010
Received in revised form 9 April 2010
Accepted 25 April 2010
Available online 16 May 2010

Keywords:
Ceramics
Oxides
X-ray diffraction
Dielectric properties

ABSTRACT

The dielectric properties and microstructures of xLa($Mg_{1/2}Ti_{1/2}$)O_3–(1 − x)$Ca_{0.6}Nd_{0.8/3}TiO_3$ ceramics with B_2O_3 additions (0.5 wt.%), prepared by the conventional solid-state route have been studied. Doping with B_2O_3 (0.5 wt.%) can effectively promote the densification and the dielectric properties of xLa($Mg_{1/2}Ti_{1/2}$)O_3–(1 − x)$Ca_{0.6}Nd_{0.8/3}TiO_3$ ceramics. It is found that xLa($Mg_{1/2}Ti_{1/2}$)O_3–(1 − x)$Ca_{0.6}Nd_{8/3}TiO_3$ ceramics can be sintered at 1400 °C, due to the liquid phase effect of B_2O_3 addition observed by Scanning Electronic Microscopy. At 1475 °C, 0.6La($Mg_{1/2}Ti_{1/2}$)O_3–0.4$Ca_{0.6}Nd_{0.8/3}TiO_3$ ceramics with 0.5 wt.% B_2O_3 addition possesses a dielectric constant (ε_r) of 39, a $Q \times f$ value of 41,000 (at 8 GHz) and a temperature coefficients of resonant frequency (τ_f) of −2.6 ppm/°C. As the content of La($Mg_{1/2}Ti_{1/2}$)O_3 increases, the highest $Q \times f$ value of 52,000 (GHz) for x = 0.8 is achieved at the sintering temperature 1475 °C.

1. Introduction

The microwave dielectric properties of La($Mg_{1/2}Ti_{1/2}$)O_3 (LMT) were previously studied and the reported values of e and $Q \times f$ are in a good mutual agreement, i.e., 27.4–29 and 63100–75500, respectively. However, there are some discrepancies in crystal structure data. In earlier papers, the structure of LMT was reported as a cubic one (space group Pa3, a = 7.9 Å or a = 3.9 Å). Later, 1/2(1 1 1) superlattice reflection and splits of the fundamental lines were observed, but no other structural information was given. Quite recently the structure was re-refined and found to have lower symmetry, but there was still a contradiction in the assigned space group. Previous studies described the structure with Pbnm space group. Further lowering of symmetry in the latter case is caused not so much by the distortion of the unit cell (β = 89.96°) but by the presence of only one B site in the Pbnm space group and therefore its inability to describe existing Mg/Ti ordering.

Using two or more compounds with negative and positive temperature coefficients to form a solid solution or mixed phases is the most promising method of obtaining a zero temperature coefficient of the resonant frequency, in our previous reports [1–3]. A previous report indicated that La($Mg_{1/2}Ti_{1/2}$)O_3–$CaTiO_3$ exhibits excellent dielectric properties at 1450 °C: an ε_r of 43.5, a $Q \times f$ of 24,000 GHz (at 8 GHz), and a τ_f of −8.9 ppm/°C [4,5]. In this work, instead of $CaTiO_3$, $Ca_{0.6}Nd_{0.8/3}TiO_3$ (CNT) (ε_r = 108, $Q \times f$ = 17,000 GHz, τ_f = +270 ppm/°C) [6] was chosen as a compensator for τ_f.

In previous studies, La($Mg_{1/2}Ti_{1/2}$)O_3 sintering temperature was as high as 1650 °C. In this work, B_2O_3 was selected as a sintering aid [7–9] to lower the sintering temperature of xLa($Mg_{1/2}Ti_{1/2}$)O_3–(1 − x)$Ca_{0.6}Nd_{0.8/3}TiO_3$ ceramics. The crystalline phases, the microstructures and the microwave dielectric properties of B_2O_3–doped xLa($Mg_{1/2}Ti_{1/2}$)O_3–(1 − x)$Ca_{0.6}Nd_{0.8/3}TiO_3$ ceramics were investigated. Mixtures of La($Mg_{1/2}Ti_{1/2}$)O_3 and $Ca_{0.6}Nd_{0.8/3}TiO_3$ ceramics were employed to obtain a new dielectric material system with a high dielectric constant, a high $Q \times f$ value and a near-zero temperature coefficient of resonant frequency. The dielectric properties and microstructures of the xLa($Mg_{1/2}Ti_{1/2}$)O_3–(1 − x)$Ca_{0.6}Nd_{0.8/3}TiO_3$ ceramic system were also evaluated.

2. Experimental procedure

Samples of xLa($Mg_{1/2}Ti_{1/2}$)O_3–(1 − x)$Ca_{0.6}Nd_{0.8/3}TiO_3$ were synthesized by conventional solid-state method. The starting materials were mixed according to a stoichiometric ratio. A small amount of B_2O_3 (0.5 wt.%) was added as a sintering aid. The starting materials were stoichiometrically weighed after drying La_2O_3 and Nd_2O_3 at 1000 °C for 24 h and MgO at 800 °C for 6 h to remove moisture content and carbonates and mixed for 24 h with distilled water. The mixture was dried at 100 °C and thoroughly milled before it was calcined at 1200 °C for 4 h. The calcined powder was ground and sieved through 100-mesh screen. Phase formation of xLa($Mg_{1/2}Ti_{1/2}$)O_3–(1 − x)$Ca_{0.6}Nd_{0.8/3}TiO_3$ was confirmed using X-ray diffraction. The calcined powders were then re-milled for 24 h with PVA solution as a binder. Pellets 11 mm in diameter and 5 mm in thickness were pressed using uniaxial pressing. A pressing pressure of 2000 kg/cm² was used for all samples. After debinding, these pellets were sintered at temperatures 1400–1500 °C for 5 h in air. The powder and bulk X-ray diffraction (XRD, Rigaku D/Max III.V) spectra were collected using Cu

* Fax: +886 6 335981.
E-mail address: cubnck@yahoo.com.tw.

0925-8388/$ – see front matter
doi:10.1016/j.jallcom.2010.04.132

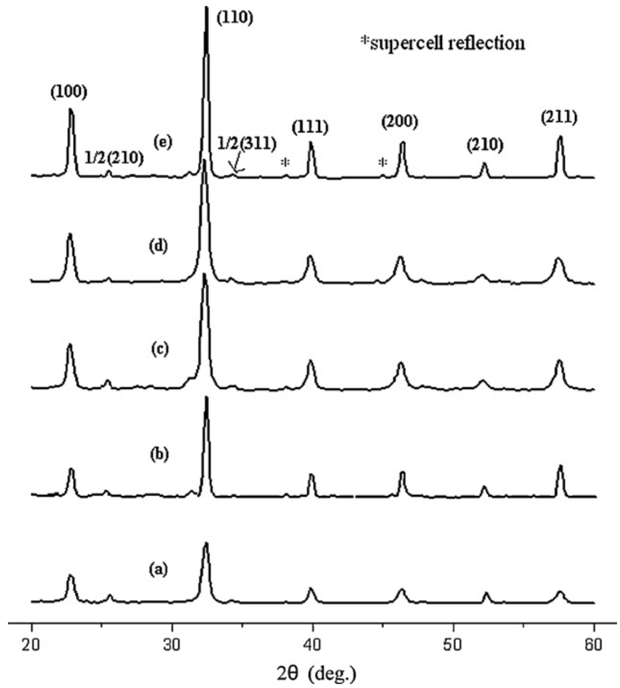

Fig. 1. X-ray diffraction patterns of 0 xLa($Mg_{1/2}Ti_{1/2}$)O_3–$(1-x)Ca_{0.6}Nd_{0.8/3}TiO_3$ ceramics with 0.5 wt.% B_2O_3 addition sintered at 1475 °C for 5 h. x = (a) 0.4 (b) 0.5 (c) 0.6 (d) 0.7 (e) 0.8.

Kα radiation (at 30 kV and 20 mA). The microstructural observations and analysis of sintered surface were performed by a scanning electron microscopy (SEM, Philips XL-40FEG).

The bulk densities of the sintered pellets were measured by the Archimedes method. The dielectric constant (ε_r) and the quality factor values (Q) at microwave frequencies were measured using the Hakki–Coleman [10] dielectric resonator method as modified and improved by Courtney [11]. The dielectric resonator was positioned between two brass plates. A system combined with a HP8757D network analyzer and a HP8350B sweep oscillator was employed in the measurement. Identical technique was applied in measuring the temperature coefficient of resonant frequency (τ_f). The test set was placed over a thermostat in the temperature range from +25 to +80 °C. The τ_f value (ppm/°C) can be calculated by noting the change in resonant frequency (Δf),

$$\tau_f = \frac{f_2 - f_1}{f_1(T_2 - T_1)} \quad (1)$$

where f_1 and f_2 represent the resonant frequencies at T_1 and T_2, respectively.

3. Results and discussion

Fig. 1 shows the X-ray diffraction patterns of 1 wt.% B_2O_3–doped xLa($Mg_{1/2}Ti_{1/2}$)O_3–$(1-x)Ca_{0.6}Nd_{0.8/3}TiO_3$ ceramics at 1475 °C. All the peaks were indexed based on the perovskite unit cell. The X-ray diffraction patterns of the xLa($Mg_{1/2}Ti_{1/2}$)O_3–$(1-x)Ca_{0.6}Nd_{0.8/3}TiO_3$ solid solution have not shown significant change with 0.5 wt.% B_2O_3 addition. Second phase was not observed at the level of 0.5 wt.% B_2O_3 addition as the detection of a minor phase by X-ray is extremely difficult. In Fig. 1, XRD patterns of La($Mg_{1/2}Ti_{1/2}$)O_3–$Ca_{0.6}Nd_{0.8/3}TiO_3$ ceramic systems form solid solution, and all peaks match with La($Mg_1Ti_{1/2}$)O_3–$Ca_{0.6}Nd_{0.8/3}TiO_3$ compound.

The spectra for all the compositions were indexed according to an orthorhombic unit cell with space group Pbnm (No. 62, cab nonstandard setting for Pnma). Combinations of odd (O) and even (E) reflections indicate a distorted perovskite structure (individual peaks are identified by numbers in brackets). On the basis of Glazer's notation, the (OOE, OEO, and EOO) reflections are assigned to an in-phase tilting of the oxygen octahedra surrounding the B-site cations. The (OOO) reflections are assigned to an antiphase tilting of the oxygen octahedra. The presence of reflections with

Table 1
xLa($Mg_{1/2}Ti_{1/2}$)O_3–$(1-x)$ $Ca_{0.6}Nd_{0.8/3}TiO_3$ cell parameters.

xLMT-$(1-x)$CNT	a (Å)	b (Å)	c (Å)	Structure
0.8LMT–0.2CNT	5.55023	5.5612	7.88121	Orthorhombic
0.7LMT–0.3CNT	5.53451	5.54721	7.85551	Orthorhombic
0.6LMT–0.4CNT	5.52012	5.53153	7.81642	Orthorhombic
0.5LMT–0.5CNT	5.50063	5.52551	7.7846	Orthorhombic
0.4LMT–0.6CNT	5.48527	5.51182	7.7785	Orthorhombic

(EEO, EOE, and OEE) combinations is associated with antiparallel displacement of A-site cations. The tilting mechanism defined by the present combination of distortions is consistent with an orthorhombic a−a−c+ tilt system [12].

As a result the La($Mg_{1/2}Ti_{1/2}$)O_3 structure adopts a monoclinic P21/n space group (No. 14) which has similar systematic absences as in Pbnm except that the 0kl: $k = 2n + 1$ condition is lifted. A disordered B-site sublattice structure is attained at $x = 0.3$, illustrated by the absence of the (0 1 1) reflection ($2\theta = 19.65°$). This is because the increase in the $Ca_{0.6}Nd_{0.8/3}TiO_3$ content in the solid solution destroys the stoichiometric 1:1 ratio of Mg:Ti ions, manifested in La($Mg_{1/2}Ti_{1/2}$)O_3 ($x = 1$), thus diminishing the condition for long-range ordering in the sublattice. However, the size and charge differences between Mg^{2+} and Ti^{4+} cations, which are the driving forces for ordering, are not changed; The lattice parameters and unit-cell volumes of La($Mg_1Ti_{1/2}$)O_3–$Ca_{0.6}Nd_{0.8/3}TiO_3$ ceramics are presented in Table 1. Employing the calculated lattice parameters (Table 1).

The SEM photographs of xLa($Mg_{1/2}Ti_{1/2}$)O_3–$(1-x)Ca_{0.6}Nd_{0.8/3}TiO_3$ ceramics sintered at 1450 °C for different x values are illustrated in Fig. 2. For all compositions, low level porosity and densed ceramic could be observed. The grain size increased with the increasing $Ca_{0.6}Nd_{0.8/3}TiO_3$ content due to its lower sintering temperature.

The SEM photographs of 0.6La($Mg_{1/2}Ti_{1/2}$)O_3–$0.4Ca_{0.6}Nd_{0.8/3}TiO_3$ ceramics sintered at various temperatures for 5 h are illustrated in Fig. 3. For all compositions, low level porosity and densed ceramic could be observed in the figure. The degree of the grain growth increased with the increase in sintering temperature. Porous specimens could not be observed for all sintered ceramics. It may play an important role to degrade the lattice vibration and get the high Q value. However, 0.6La($Mg_{1/2}Ti_{1/2}$)O_3–$0.4Ca_{0.6}Nd_{0.8/3}TiO_3$ inhomogeneous grain growth was observed at temperatures higher than 1500 °C with 0.5 wt.% B_2O_3 additive, which might degrade the microwave dielectric properties of the ceramics. The inhomogeneous rod-like grains were identified, in all samples. It is possible to evaluate the effect of grain orientation on the XRD patterns as can be seen from Fig. 1 and in Fig. 3 have lattice constant vibrational. At 1500 °C, the phenomenon of abnormal grain growth occurs in soap foams and polycrystalline ceramics for example. The driving force in these systems is the surface tension which leads to a reduction in the total surface area of the grains. Grain growth is the process that takes place during annealing of polycrystalline materials; its major feature is a systematic increase in grain size. Two different types of grain growth can be distinguished: the normal and abnormal grain growth. On the contrary, when the abnormal grain growth is the dominant mechanism, there are certain grains (abnormal grains) in the microstructure that grow much faster than the majority of the grains and in the end consume the fine-grained matrix around them. There has been a lot of work done in the field of abnormal grain growth, but the actual mechanism of abnormal grain formation and development from a uniform grain size distribution is not fully understood.

The density of the B_2O_3-doped 0.6La($Mg_{1/2}Ti_{1/2}$) O_3–$0.4Ca_{0.6}Nd_{0.8/3}TiO_3$ ceramics at differential sintering

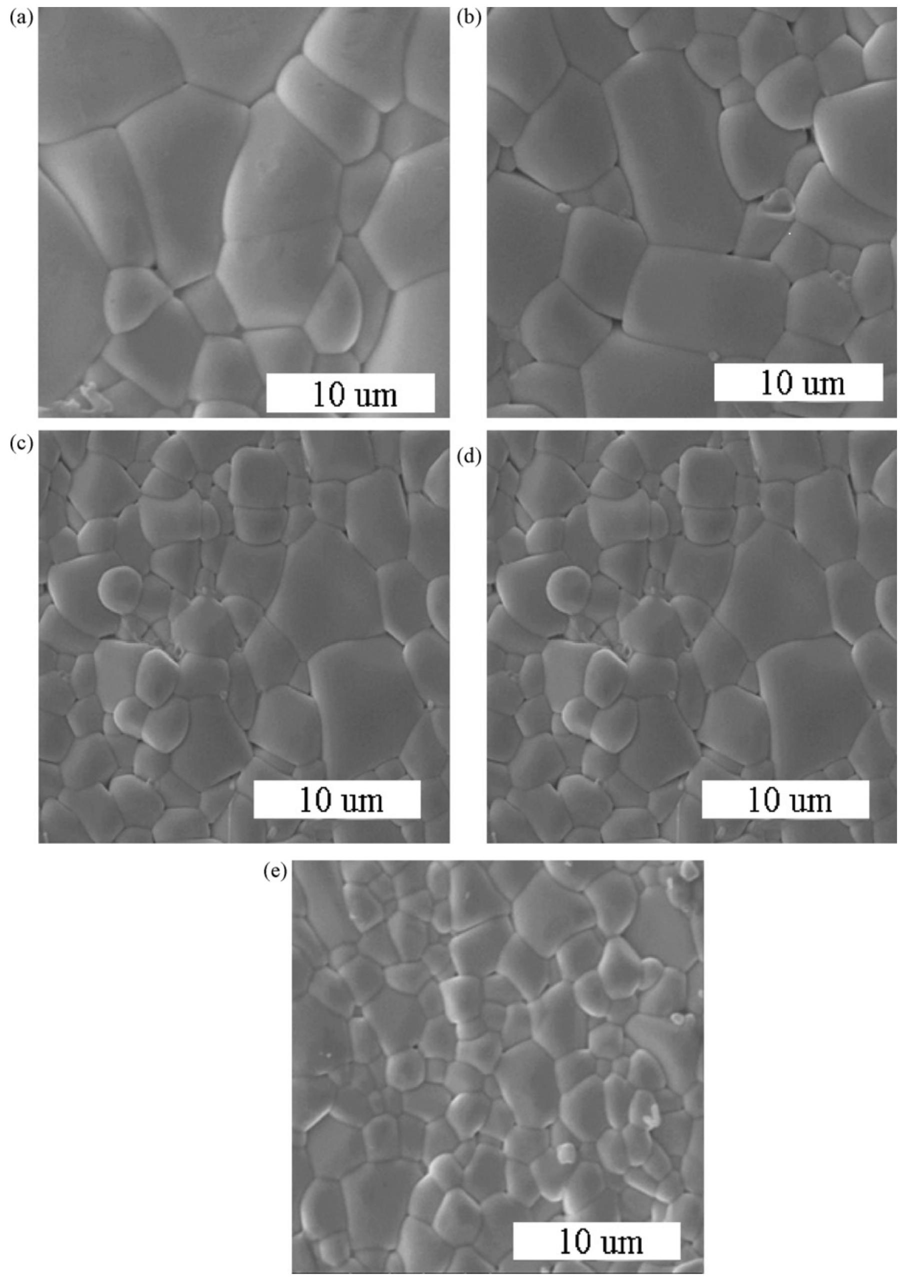

Fig. 2. SEM photographs of xLa($Mg_{1/2}Ti_{1/2}$)O_3–(1 − x) $Ca_{0.6}Nd_{0.8/3}TiO_3$ ceramics (a) x = 0.4, (b) x = 0.5, (c) x = 0.6 (d) x = 0.7 and (e) x = 0.8 with 0.5 wt.% B_2O_3 additions sintered at 1450 °C for 5 h.

temperature is shown in Fig. 4. It indicated that densities of 5.6–5.1 (g/cm^3) were obtained for B_2O_3-doped 0.6La($Mg_{1/2}Ti_{1/2}$)O_3–0.4$Ca_{0.6}Nd_{0.8/3}TiO_3$ ceramics at sintering temperatures from 1400 to 1500 °C. The density increased with increasing sintering temperature due to enlarged grain size as observed in Fig. 3, and was also affected by the composition and decreased with increasing x value. It suggested that more $Ca_{0.6}Nd_{0.8/3}TiO_3$ content and sintering at higher temperatures (above 1475 °C owing to the over-sintering) would degrade the bulk density of the ceramics.

The dielectric properties of xLa($Mg_{1/2}Ti_{1/2}$)O_3–(1 − x)$Ca_{0.6}Nd_{0.8/3}$ TiO_3 with 0.5 wt.% B_2O_3 addition are illustrated in Fig. 5. As the x value increased from 0.4 to 0.8, the dielectric constants decreased from 46 to 29. 0.6La($Mg_{1/2}Ti_{1/2}$)O_3–0.4$Ca_{0.6}Nd_{0.8/3}TiO_3$ dielectric constants slightly decreased with increasing the sintering temperature above 1450 °C. The decrease in ε_r value with increasing sintering temperature could be explained owing to the over-sintering of xLa($Mg_{1/2}Ti_{1/2}$)O_3–(1 − x)$Ca_{0.6}Nd_{0.8/3}TiO_3$. With 0.5 wt.% B_2O_3 addition, a ε_r value of 40 was obtained for 0.6La($Mg_{1/2}Ti_{1/2}$)O_3–0.4$Ca_{0.6}Nd_{0.8/3}TiO_3$ ceramics sintered at 1450 °C.

Fig. 6 shows the $Q \times f$ values of xLa($Mg_{1/2}Ti_{1/2}$) O_3–(1 − x)$Ca_{0.6}Nd_{0.8/3}TiO_3$ ceramics with 0.5 wt.% B_2O_3 additions at different sintering temperatures as functions of the x value. The $Q \times f$ value increase with the increase in La($Mg_{1/2}Ti_{1/2}$)O_3 content and sintering temperature. It was expected as the quality factor of La($Mg_{1/2}Ti_{1/2}$)O_3 is much higher than that of $Ca_{0.6}Nd_{0.8/3}TiO_3$ and the bulk density increased with increasing sintering temperature due to the ceramics being denser. Many factors could affect the microwave dielectric loss of dielectric resonators such as the lattice vibration modes, the pores and the secondary phases. Generally, a larger grain size, i.e., a smaller grain boundary, indicates a reduction in lattice imperfection and the dielectric loss was thus reduced. It seems that

(a)
(b)
(c)
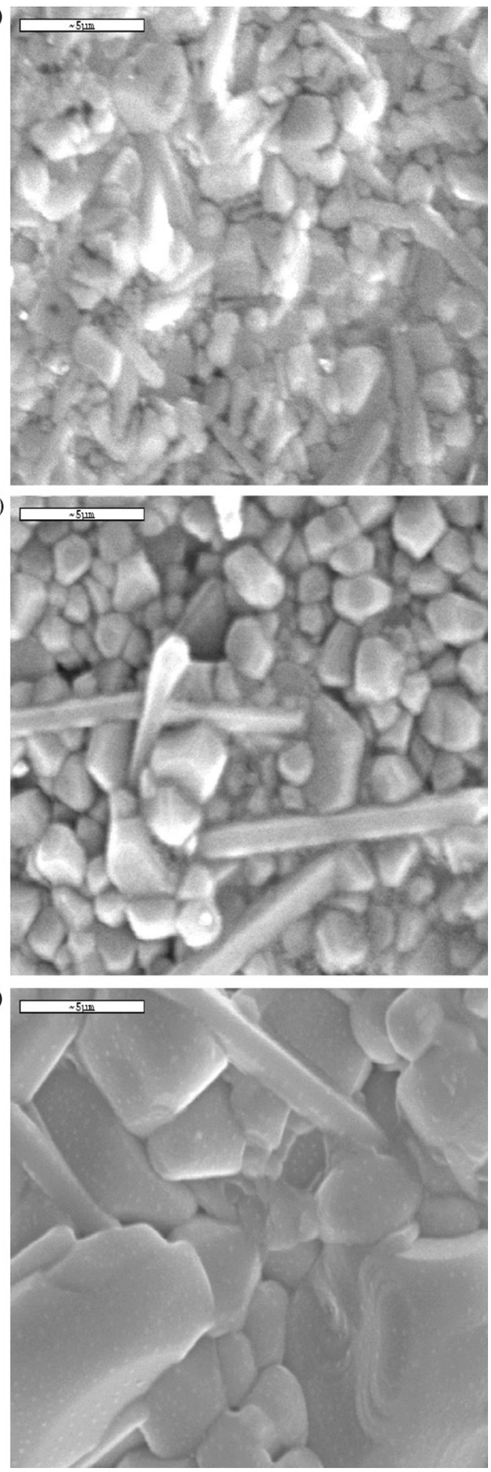

Fig. 3. SEM photographs of 0.6La$(Mg_{1/2}Ti_{1/2})O_3$–0.4$Ca_{0.6}Nd_{0.8/3}TiO_3$ ceramics sintered at (a) 1400 °C, (b) 1450 °C and (c) 1500 °C with 0.5 wt.%B_2O_3 additions for 5 h.

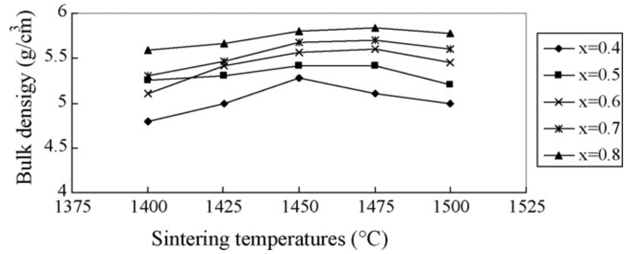

Fig. 4. Bulk density of xLa$(Mg_{1/2}Ti_{1/2})O_3$–$(1-x)Ca_{0.6}Nd_{0.8/3}TiO_3$ ceramics system sintered at different temperatures with 0.5 wt.% B_2O_3 addition.

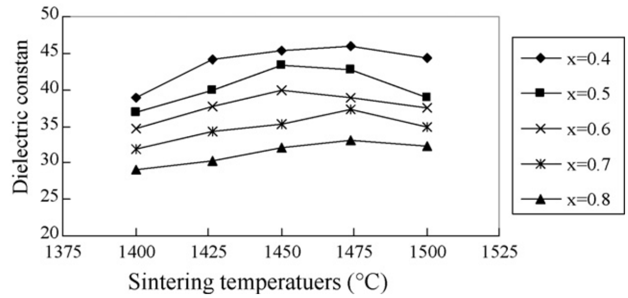

Fig. 5. ε_r value of xLa$(Mg_{1/2}Ti_{1/2})O_3$–$(1-x)Ca_{0.6}Nd_{0.8/3}TiO_3$ ceramics system sintered at different temperatures with 0.5 wt.% B_2O_3 addition.

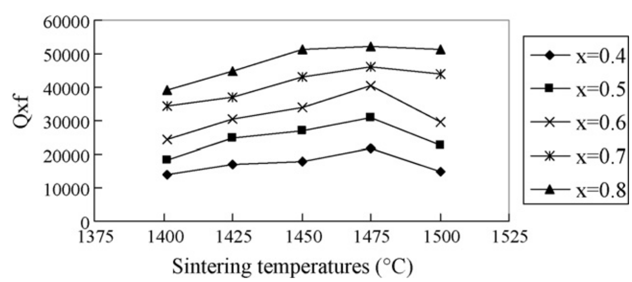

Fig. 6. $Q \times f$ value of xLa$(Mg_{1/2}Ti_{1/2})O_3$–$(1-x)Ca_{0.6}Nd_{0.8/3}TiO_3$ ceramics system sintered at different temperatures with various 0.5 wt.% B_2O_3 addition.

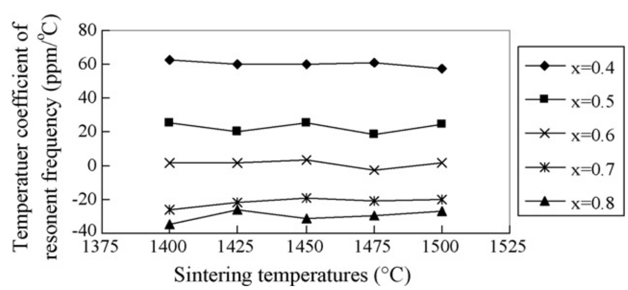

Fig. 7. Temperature coefficient value of xLa$(Mg_{1/2}Ti_{1/2})O_3$–$(1-x)Ca_{0.6}Nd_{0.8/3}TiO_3$ ceramics system sintered at different temperatures with 0.5 wt.% B_2O_3 addition.

the dielectric loss of xLa$(Mg_{1/2}Ti_{1/2})O_3$–$(1-x)Ca_{0.6}Nd_{0.8/3}TiO_3$ ceramics system was dominated by the bulk density and the grain size. $Q \times f$ value of 41,000 (GHz) was obtained for 0.6La$(Mg_{1/2}Ti_{1/2})O_3$–0.4$Ca_{0.6}Nd_{0.8/3}TiO_3$ ceramics at 1475 °C for 4 h.

The temperature coefficients of resonant frequency (τ_f) of B_2O_3-doped xLa$(Mg_{1/2}Ti_{1/2})O_3$–$(1-x)Ca_{0.6}Nd_{0.8/3}TiO_3$ ceramics at different sintering temperatures are illustrated in Fig. 7. The temperature coefficient of resonant frequency is well known related to the composition, the additives and the second phase of the material. It seemed that higher $Ca_{0.6}Nd_{0.8/3}TiO_3$ content would shift the τ_f value to more positive. It varied from −29.6 to 61 ppm/°C as the amount of $Ca_{0.6}Nd_{0.8/3}TiO_3$ addition increased from 0.4 to 0.8 sintered at 1475 °C. In general, the temperature coefficient of resonant frequency was found to be related to the composition and the existing phase in ceramics.

In our previous studies, at 1450 °C, 0.5 La$(Mg_{1/2}Ti_{1/2})$ O_3–0.5$CaTiO_3$ ceramics with 0.25 wt.% B_2O_3 additive have a dielectric constant (ε_r) of 43, a $Q \times f$ value of 24470 (at 8 GHz) and a temperature coefficient of resonant frequency (τ_f) of

−8.94 ppm/°C [13]. So, xLa($Mg_{1/2}Ti_{1/2}$)O_3–(1 − x)$Ca_{0.6}Nd_{0.8/3}TiO_3$ ceramics exhibited better dielectric properties. With 0.5 wt.% B_2O_3 addition, a dielectric constant of 39, a $Q \times f$ value of 41,000 (GHz) and a τ_f value of −2.6 ppm/°C were obtained for 0.6La($Mg_{1/2}Ti_{1/2}$)O_3–0.4$Ca_{0.6}Nd_{0.8/3}TiO_3$ ceramics at 1475 °C for 4 h.

4. Conclusion

The dielectric properties of B_2O_3–doped xLa($Mg_{1/2}Ti_{1/2}$)O_3–(1 − x)$Ca_{0.6}Nd_{0.8/3}TiO_3$ ceramics were investigated. xLa($Mg_{1/2}Ti_{1/2}$)O_3–(1 − x)$Ca_{0.6}Nd_{0.8/3}TiO_3$ ceramics exhibited perovskite structure. With 0.5 wt.% B_2O_3 addition, a dielectric constant of 39, a $Q \times f$ value of 41,000 (GHz) and a τ_f value of −2.6 ppm/°C were obtained for 0.6La($Mg_{1/2}Ti_{1/2}$)O_3–0.4$Ca_{0.6}Nd_{0.8/3}TiO_3$ ceramics at 1475 °C for 4 h. Therefore, the B_2O_3-doped xLa($Mg_{1/2}Ti_{1/2}$)O_3–(1 − x)$Ca_{0.6}Nd_{0.8/3}TiO_3$ ceramic is suitable for applications in microwave dielectric resonators and microwave device because of its excellent microwave dielectric properties.

References

[1] C.-L. Huang, Y.-B. Chen, C.-F. Tasi, J. Alloys Compd. 460 (2008) 675–679.
[2] C.L. Huang, Y.-B. Chen, C.-F. Tasi, J. Alloys Compd. 454 (2008) 454–459.
[3] C.-L. Huang, C.-F. Tasi, Y.-B. Chen, Y.-C. Cheng, J. Alloys Compd. 453 (2008) 337–340.
[4] S.-Y. Cho, C.-H. Kim, D.-W. Kim, Mater. Res. Soc. 14 (1999) 2484.
[5] C.-L. Huang, Y.-B. Chen, C.-W. Lo, Jpn. J. Appl. Phys. 44 (2005) 3147–3150.
[6] C.-L. Huang, J.-T. Tsai, Y.-B. Chen, Mater. Res. Bull. 36 (2001) 54.
[7] T. Takada, S.F. Wang, S. Yoshikawa, S.-J. Jang, R.E. Newnham, J. Am. Ceram. Soc. 77 (1994) 2485.
[8] S. Hirno, T. Hayashi, A. Hattori, J. Am. Ceram. Soc. 74 (1991) 1320.
[9] V. Tolmer, G. Desgardin, J. Am. Ceram. Soc. 80 (1997) 1981.
[10] B.W. Hakki, P.D. Coleman, IEEE Trans. Microwave Theory Tech. 8 (1960) 402.
[11] W.E. Courtney, IEEE Trans. Microwave Theory Tech. 18 (1970) 476.
[12] E.R. Kipkoech, F. Azough, R. Freer, J. Appl. Phys. 97 (2005) 064103.
[13] C.-L. Huang, Y.-B. Chen, C.-W. LO, Jpn. J. Appl. Phys. 44 (2005) 3147–3150.